SINTEF
PROCEEDINGS
2

Proceedings of the 12th International Conference on Computational Fluid Dynamics in the Oil & Gas, Metallurgical and Process Industries

Progress in Applied CFD – CFD2017

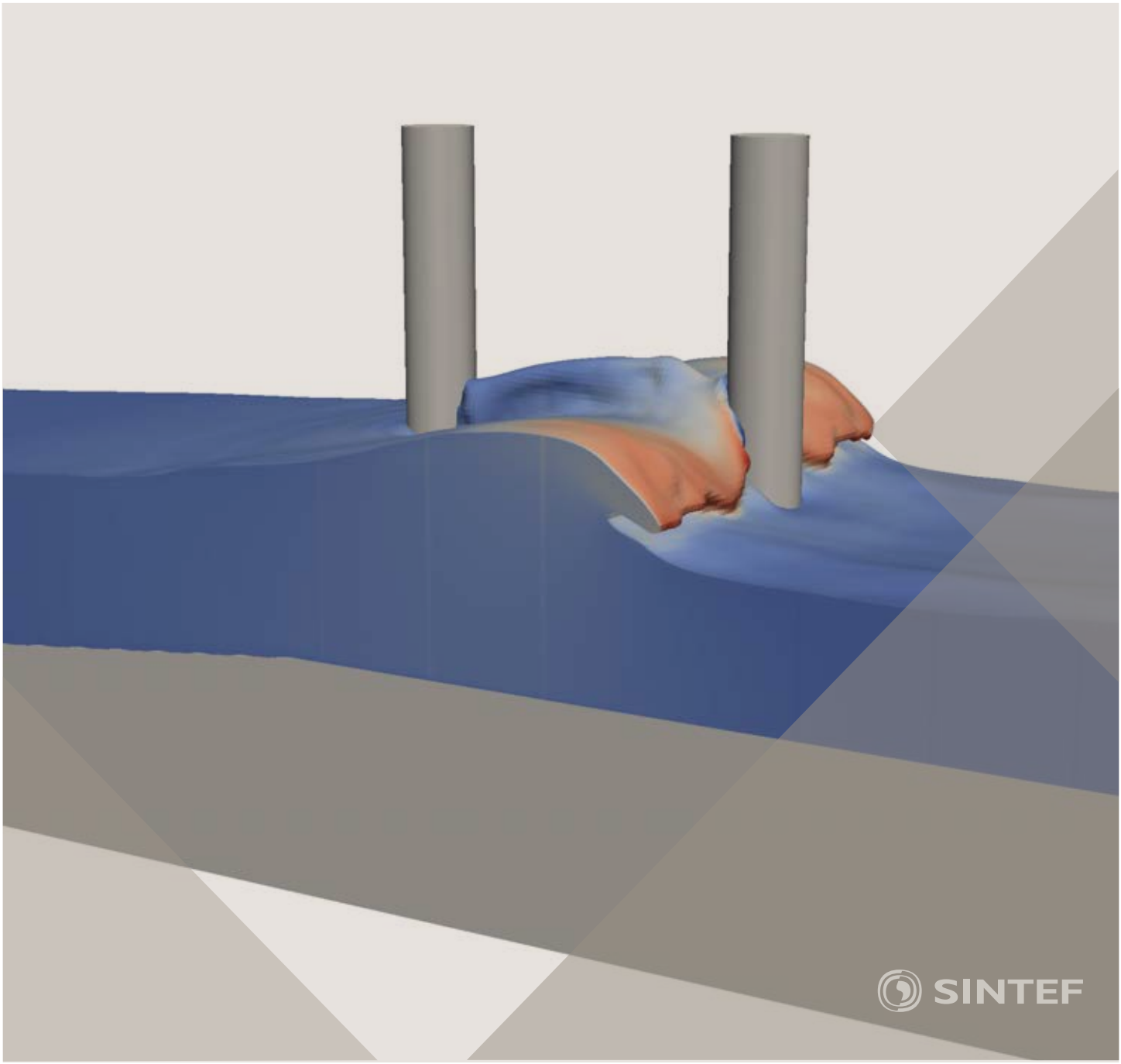

SINTEF Proceedings

Editors:
Jan Erik Olsen and Stein Tore Johansen

Progress in Applied CFD – CFD2017

Proceedings of the 12th International Conference on Computational Fluid Dynamics in the Oil & Gas, Metallurgical and Process Industries

SINTEF Academic Press

SINTEF Proceedings no 2
Editors: Jan Erik Olsen and Stein Tore Johansen
Progress in Applied CFD – CFD2017
Selected papers from 10th International Conference on Computational Fluid Dynamics in the Oil & Gas, Metallurgical and Process Industries

Key words:
CFD, Flow, Modelling

Cover, illustration: Arun Kamath

ISSN 2387-4295 (online)
ISBN 978-82-536-1544-8 (pdf)

SINTEF Academic Press
Address: Forskningsveien 3 B
PO Box 124 Blindern
N-0314 OSLO
Tel: +47 73 59 30 00
Fax: +47 22 96 55 08

www.sintef.no/byggforsk
www.sintefbok.no

SINTEF Proceedings
SINTEF Proceedings is a serial publication for peer-reviewed conference proceedings on a variety of scientific topics.
The processes of peer-reviewing of papers published in SINTEF Proceedings are administered by the conference organizers and proceedings editors. Detailed procedures will vary according to custom and practice in each scientific community.

PREFACE

This book contains all manuscripts approved by the reviewers and the organizing committee of the 12th International Conference on Computational Fluid Dynamics in the Oil & Gas, Metallurgical and Process Industries. The conference was hosted by SINTEF in Trondheim in May/June 2017 and is also known as CFD2017 for short. The conference series was initiated by CSIRO and Phil Schwarz in 1997. So far the conference has been alternating between CSIRO in Melbourne and SINTEF in Trondheim. The conferences focuses on the application of CFD in the oil and gas industries, metal production, mineral processing, power generation, chemicals and other process industries. In addition pragmatic modelling concepts and bio-mechanical applications have become an important part of the conference. The papers in this book demonstrate the current progress in applied CFD.

The conference papers undergo a review process involving two experts. Only papers accepted by the reviewers are included in the proceedings. 108 contributions were presented at the conference together with six keynote presentations. A majority of these contributions are presented by their manuscript in this collection (a few were granted to present without an accompanying manuscript).

The organizing committee would like to thank everyone who has helped with review of manuscripts, all those who helped to promote the conference and all authors who have submitted scientific contributions. We are also grateful for the support from the conference sponsors: ANSYS, SFI Metal Production and NanoSim.

Stein Tore Johansen & Jan Erik Olsen

Organizing committee:

Conference chairman: Prof. Stein Tore Johansen
Conference coordinator: Dr. Jan Erik Olsen
Dr. Bernhard Müller
Dr.Sigrid Karstad Dahl
Dr.Shahriar Amini
Dr.Ernst Meese
Dr.Josip Zoric
Dr.Jannike Solsvik
Dr.Peter Witt

Scientific committee:

Stein Tore Johansen, SINTEF/NTNU
Bernhard Müller, NTNU
Phil Schwarz, CSIRO
Akio Tomiyama, Kobe University
Hans Kuipers, Eindhoven University of Technology
Jinghai Li, Chinese Academy of Science
Markus Braun, Ansys
Simon Lo, CD-adapco
Patrick Segers, Universiteit Gent
Jiyuan Tu, RMIT
Jos Derksen, University of Aberdeen
Dmitry Eskin, Schlumberger-Doll Research
Pär Jönsson, KTH
Stefan Pirker, Johannes Kepler University
Josip Zoric, SINTEF

CONTENTS

DEVELOPMENT OF GPU PARALLEL MULTIPHASE FLOW SOLVER FOR TURBULENT SLURRY FLOWS IN CYCLONE

Kumar MAYANK[1]*, **Raja BANERJEE**[2]†, **Narasimha MANGADODDY**[1]‡

[1]IIT Hyderabad Department of Chemical Engineering, 502285 Medak, India

[2]IIT Hyderabad Department of Mechanical Engineering, 502285 Medak, India

* E-mail: ch15resch02001@iith.ac.in
† E-mail: rajabanerjee@iith.ac.in
‡ E-mail: narasimha@iith.ac.in

ABSTRACT

The development of GPU parallelized unstructured multiphase solver and its application in predicting turbulent swirling flow of slurries inside cyclones is presented. Algebraic slip mixture model (ASM) is modified with additional shear lift forces and slurry rheology is corrected with fines fraction. The modified ASM model coupled with LES is used to predict particle classification inside hydrocyclone. During hydrocyclone operation the residence time of the fluid is very small and hence there is insufficient time for the larger eddies to cascade into smaller eddies. LES can accurately resolve flow structures that are few times the Kolmogorov scale at an increased computational cost due to finer mesh requirement. Therefore, the solver has been parallelized using general purpose graphics processing units (GPGPUs). In the current solver, the Pressure Poisson equation has been parallelized with an algebraic multigrid solver on GPU architecture using CUDA programming language for unstructured grids. The single phase flow field predicted by LES shows good agreement with experimental results obtained from open literature. The turbulent flow fields, the size segregation and the particle efficiency curve obtained from multiphase simulations are presented. Additionally, computational speedup due to GPU parallelization is reported over its serial version of the solver.

Keywords: CFD, hydrodynamics, LES, GPU, ASM .

NOMENCLATURE

A complete list of symbols used, with dimensions, is required.

NOMENCLATURE

Greek Symbols
ρ_m Mixture density, $[kg/m^3]$
μ_c viscosity of the continuous phase, $[kg/ms]$.
μ_m viscosity of the mixture, $[kg/ms]$.
α_k Volume fraction of phase.
α_p Total particle volume fraction.
α_{pm} Maximum packing fraction.
ω_{mj} Vorticity vectors.
ε_{ijk} Kronecker delta.

Other Symbols
p Pressure, $[Pa]$.
$\mathbf{u}_m$ Mixture velocity, $[m/s]$.
$\mathbf{u}_{cp}$ Slip velocity for phase p, $[m/s]$.
d_p diameter of the particle,$[m]$.
Re_p Reynolds number of the particle.
C_{lp} lift coefficient.
S_f Face area vector.
F_f mass flux through face f.

Sub/superscripts
i, j Spatial coordinate index .
k Phase Index.
f Face Index .

INTRODUCTION

The use of computational fluid dynamics(CFD) for design exploration has been prevalent for the past couple of decades. Most of these studies have relied on RANS based approach to model the entire range of turbulence length scales in the flow. Though computationally efficient RANS based approach fail to account for the dynamic interactions between the large and small scales of motion, and has been observed to have limited predictive capabilities for decay of isotropic turbulence even in simpler configurations(Pope, 2004). With the availability of increased computational power recently, LES and DNS have been used extensively to model turbulence in complex flow configuration. While, DNS typically resolves all turbulence length scales down to the smallest Kolmogorov scale. LES uses a spatial filter to separate the larger scale motions from the smaller scales. The larger scales of motion are anisotropic and LES resolves all the scales above the specified cutoff length. While using a sub-grid scale model (Germano *et al.*, 1991; Lilly, 1992) to incorporate the effects of the small scale motions on the resolved scales. This feature makes LES much less computationally extensive as compared to DNS where even the universally isotropic smaller scales(Leonard, 1975) are resolved, requiring mesh resolution in the order of $Re^{9/4}$ for DNS computations. LES has been reported to have good turbulence predictive capabilities for channel flow (Deardorff, 1970; Moin and Kim, 1982), recirculating flows (Kobayashi, 1992) as well as in complex flow configuration such as in gas turbine combustion (Moin and Apte, 2006). LES has been used to simulate highly strained flows in complex geometries was first performed by (Slack *et al.*, 2000) and since has been used to predict flow dynamics inside hydrocyclones(Brennan, 2006) as well as predicting the cut size(Narasimha *et al.*, 2006).

The comparatively high mesh requirement for LES as compared to RANS based models is the major drawback that limits the scope of LES simulations for design exploration at realistic industrial configurations. Using general purpose GPU for parallelizing linear equation solvers was explored by (Sanders and Kandrot, 2010) and further development for method of parallelisation for unstructured and hybrid mesh solvers was presented in (Xu *et al.*, 2014) and for two phase flow problems in(Reddy and Banerjee, 2015). The massive parallel compute capability of the GPU allows conducting high fidelity LES simulations for industrial configurations computationally feasible.

The work presented in this study explains the development of a high fidelity LES multiphase solver using the algebraic slip model to study flow of poly dispersed slurry system. The solver was parallelized by porting the pressure poisson equation solver on the GPU. The single phase LES solver is validated against LDA measurements for cyclone flows reported in open literature. The multiphase code is tested for particle segregation inside a hydrocyclone. The cut point predicted by the multiphase code was found to be agreeable with the simulation results presented in literature. Finally the speed up obtained for parallel implementation over serial version is reported in the final section.

MODEL DESCRIPTION

The slurries consists of mixture of poly dispersed solid particles within a continuous phase mostly water. The governing equation for multiphase fluid flow following (Ishii 1975) notations is given by

Continuity equation

$$\frac{\partial \rho_m}{\partial t} + \frac{\partial \rho_m u_{mi}}{\partial x_i} = 0 \tag{1}$$

Momentum Equation

$$\frac{\partial \rho_m u_{mi}}{\partial t} + \frac{\partial \rho_m u_{mi} u_{mj}}{\partial x_j} = \frac{\partial p}{\partial x_i} + \frac{\partial}{\partial x_j}(\tau_{\mu,ij} + \tau_{D,ij}) + \rho_m g_i \tag{2}$$

where the density and the velocity of the mixture is given by farve-averaged quantities explained in (Soo 1990).

$$\rho_m = \sum_{k=1}^{n} \alpha_k \rho_k \tag{3}$$

$$u_m = \frac{1}{\rho_m} \sum_{k=1}^{n} \alpha_k \rho_k u_k \tag{4}$$

Each dispersed phase is tracked using a scalar transport equation of the form

$$\frac{\partial}{\partial t}\alpha_k + \nabla \cdot (\alpha_k u_m) = -\nabla \cdot (\alpha_k u_{Mk}) \tag{5}$$

The viscous diffusive flux for the mixture ($\tau_{\mu,ij}$) is calculated using model by (Ishii-Mishima 1980) as

$$\mu_m = \mu_c (1 - \frac{\alpha_p}{\alpha_{pm}})^{-2.5\alpha_{pm}} \tag{6}$$

The extra term in the Eq. 2, ($\tau_{D,ij}$) is the diffusion flux arising due to phase slip and is given by

$$\tau_{D,ij} = -\sum_{k=1}^{n} \alpha_k \rho_k u_{mk} u_{mk} \tag{7}$$

The phase diffusion velocity u_{Mk}, is represented in terms of individual phase slip velocity as

$$u_{mp} = u_{cp} - \sum_{k=1}^{n} \alpha_k u_{ck} \tag{8}$$

The individual phase slip velocity using force balance on the particles experiencing drag was derived by (Manninen and Taivassalo, 1996) and extended to include the effects of lift forces by (Narasimha *et al.*, 2007) and is given by

$$u_{cpi} = \frac{{d_p}^2(\rho_k - \rho_m)}{18 f_{Rep} \mu_c}\left(g_i - \frac{\partial}{\partial t}u_{mi} - u_{mj}\frac{\partial}{\partial x_j}u_{mi} + 0.75\frac{\rho_c}{\rho_k - \rho_m} C_{lp} \varepsilon_{ijk} \omega_{mj} u_{pck}\right) \tag{9}$$

Where the term f_{Rep} is given by

$$f_{Rep} = (1 + 0.15 {Re_p}^{0.687})\alpha_p^{-4.65}$$

$$Re_p = \frac{d_p \rho_c |u_{cp}|}{\mu_m}$$

Numerical Implementation

The solver presented is capable of handling unstructured grid in CGNS format. Unstructured grids are preferred for industrial applications as the complex equipment geometry can be represented much easier as compared to structured grid arrangement. The implementation of numerical schemes for unstructured grids are complicated though, with increased and random inter-dependence of grid point variables. The geometric and neighbor data information of each cell is stored before the start of the solution. A collocated grid arrangement (Date, 2005) is used wherein all the solution variables are stored at the cell centers. Finite volume method is used to discretize the governing equation on the grid. A first order explicit scheme was used for the temporal term. A combination of first order and central difference scheme with the deferred correlation approach (Khosla and Rubin, 1974) was used to approximate the convective fluxes. Volumetric interpolation was used to calculate the face center values from the stored cell center variables. The diffusive fluxes and other terms are approximated in a similar method as followed by (Dalal *et al.*, 2008). The pressure correction method (Davidson, 1996) was used for the pressure velocity decoupling. The diffusive flux due to phase slip is implemented as a volumetric source term. The starting point of the solver is to initialize the grid points, initial and boundary conditions. In case of a velocity inlet both the primary phase and the secondary phase velocity as well as volume fraction for each secondary phases are specified. The solver then proceeds to calculate the density and mixture velocities at each boundary using eq. 3 and 4. These calculated mixture properties act as the actual boundary values for the solution. The mass flux for the mixture is calculated with the divergent field velocity obtained by solving the discrete form of eq. 2 without the pressure term. Then we solve the pressure poisson equation using the calculated mass flux value which is of the form.

$$\sum_f (\nabla {p_f}^{n+1}).S_f = \frac{\rho}{\Delta t}\sum_f {F_f}^* \tag{10}$$

Finally the mass flux is corrected by subtracting the pressure gradient term from the initially calculated mass flux and the divergent free velocity is obtained for the new time step. The discrete form of the phase tracking eq. 5 is then solved and

density and viscosity values are updated using eq. 6.Slip velocity is calculated with the difference between the primary and secondary phase velocities as initial guess. We calculate the term f_{Rep} which is used to calculate the individual slip velocity using eq. 9 iteratively as long as the final value reaches the desired convergence criterion. The slip velocities are used to calculate the phase diffusion velocity using eq. 8. Finally the diffusion flux due to phase slip is calculated using eq. 7, gradient of which is stored as the source term for the next time step. The gradient of the volume flux of the scalar is stored to be as the source term for the scalar transport equation for the next time step. The algorithm of the solver is explained below

Initialization:
Initialize grid points, initial and boundary condition;
Calculate mixture velocity and density boundary values;
Solution:
while *T<Final Time* **do**
  Calculate mass velocity (u*) and the mass flux for each face(F*);
  Solve pressure poisson equation using the mass flux(F*);
  Correct velocities (u^{n+1}) and flux(F^{n+1}) value using pressure correction;
  Solve the phase tracking equations;
  Update density and viscosity Calculate the slip velocities for each phase;
  Calculate the source terms for the momentum and phase tracking equation for the next time step;
end

Algorithm 1: Algorithm of the solver

GPU PARALLELIZATION

A standard V-cycle algebraic multigrid (AMG) implementation was used for solving the pressure poisson equation. The equation is of the form $Au = f$ with the coefficient matrix(A) being a symmetric matrix with six dominant diagonals. Instead of working on one mesh AMG uses a hierarchy of mesh, which are starts from the finest mesh and uses the coarsening algorithm suggested by (Haase *et al.*, 2010) to construct levels of coarser mesh. For each level the coefficient matrix(A_c), the prolongation matrix(P) and the restriction matrix(P^T) are populated. For a two level multigrid system which can be extended to multilevel system the algorithm can be summarized as

- Compute estimate $u\star$ for u in $Au = f$;
- Compute the residual $r = f - Au\star = Ae$;
- Solve for e_c in the coarser system $A_c e_c = P^T r$;
- Correct $u\star \leftarrow u\star + Pe_c$.

CUDA programming module was used to implement the AMG solver on the GPU. The implementation is rather difficult for unstructured meshes as the interdependencies between the nodes are not in an ordered arrangement. The interdependencies of the nodes though irregular, remains constant for non deforming grids. Therefore, the neighbor element data is stored at the start of the solution. Greedy coloring scheme (Hege and Stuben, 1991) was used to identify set of independent nodes. Each independent set of nodes are assigned a color class. The total number of color class was referred to as maximum degree. Which for tetrahedral element meshes comes out to be six independent sets. The nodes are updated in order of color class. Updating all the independent set of nodes simultaneously helps preventing any unrealistic solutions due to data race condition. The nodes are ordered in such a way that inter dependent nodes can be co located resulting in a coalesced memory access pattern thereby reducing the time required for the data transfer operations. Gauss Seidel method is used for the smoothening operation. In CUDA terminology, the CPU is referred to as the host and the GPU is referred to as the device. The device function is called a kernel and is identified by `__global__` identifier. The kernel is called, and the number of threads to be launched is specified from the host code. The number of threads to be launched is specified in terms of grids and blocks. For the current implementation we use grid size equal to the maximum degree and the block size is equal to the maximum number of cells within a color class. We use V-cycle multigrid, which is made up of a down cycle and up cycle. Down cycle is a sequence of smoothing and restriction operations performed alternately starting from finest grid till we reach coarsest grid. Up cycle is a combination of prolongation and smoothing operations performed alternately starting with the coarsest grid till we reach finest grid. The multigrid V-cycle is repeated till the desired convergence is reached. The algorithm for the parallelization code for the solution of the equation of the form $Ax = B$ is given in algorithm 2.

RESULTS

The parallel solver was tested for two cases. First is the single phase LES prediction for flow in industrial flow configuration within a gas cyclone. Second being the multiphase flow prediction of phase segregation under turbulent slurry flow conditions. The simulation setup and results are presented in the subsections below

Validation of LES solver

The single phase LES solver is tested for the flow configuration similar to the one presented in (Slack *et al.*, 2000). The dimensions of the geometry and the mesh used is given in the figure 1. Air with density 1.225 kg/m^3 and viscosity $1.78943 \times 10^{-5} kg.m^{-1}s^{-1}$ was used to define the fluid properties. For the cyclone volume of 0.0203 m^3 around 6.5 $\times 10^5$ hexahedral cells were used to discretize the flow domain. The inlet, overflow and the underflow are the boundary patches composed of quadrilateral cells. The inlet air flow rate was maintained at 0.08 kg/m^3, the residence time at this flow rate was 0.25 s. The pressure at the overflow was specified as gauge pressure and the velocity was specified homogeneous neumann boundary condition, whereas the underflow was specified wall boundary condition. The time step size was 1×10^{-5} s. The mean velocity magnitude, axial velocity and tangential velocity profile along the central plane is given in figure 2. Velocity magnitude profile shows an increase in the magnitude as we proceed from the walls to the central axis, while the central core is the region of lowest magnitude. Typically fluid stream upon entering the cyclone moves along the outer wall while descending down, then accelerating due to the constriction of the area and reaches the bottom wall where the flow reversal happens and the stream moves towards the exit overflow.Vortex formation can be observed due to low dynamic pressure in the

Host Code:
Populate Coefficient matrix(A), Initial Guess pressure matrix(x) and RHS matrix(b) ;
Create levels of multigrid ;
for $i = 0;\ i < number\ of\ levels:\ i++$ **do**
  Calculate $A_p[i]$, $P[i]$ and $P^T[i]$;
  Color the nodes using procedure explained by (Hege and Stuben, 1991);
  Rearrange the node for interdependent nodes to be collocated;
  Transfer data from the host to the device;
end
Device Code:
while $residual \geq convergence\ criterion$ **do**
  for $Numlevel = 1;\ Numlevel < MaxNumlevel;\ Numlevel{+}{+}$ **do**
    Calculate the residual for the finer mesh ($NumLevel - 1$) level using kernel calculateResiduals() ;
    Update the residual at the coarse level($NumLevel$) using kernel updateResiduals();
    for $ClrId = 0; ClrId < MaxDegree - 1; ClrId{+}{+}$ **do**
      Smooth the error on the coarse mesh level($NumLevel$) for color class ClrId using $gaussSiedeliteration()$ kernel;
    end
  end
  for $Numlevel$=$MaxNumlevel\text{-}2;\ Numlevel > 0;\ Numlevel{-}{-}$ **do**
    Update the pressure of the coarse mesh level($Numlevel + 1$) $updatepressure()$ kernel;
    for $ClrId = 0; ClrId < MaxDegree - 1; ClrId{+}{+}$ **do**
      Smooth the error on the coarse mesh level($Numlevel$) for the color class ClrId using $gaussSiedeliteration()$ kernel;
    end
  end
  for $ClrId = 0;\ ClrId < MaxDegree\text{-}1;\ ClrId{+}{+}$ **do**
    Smooth the error on the finest mesh level(0) using $gaussSiedeliteration()$ kernel;
  end
  Calculate the residuals for the finest mesh level(0);
end

Algorithm 2: Parallelization of standard V cycle algebraic multigrid solver

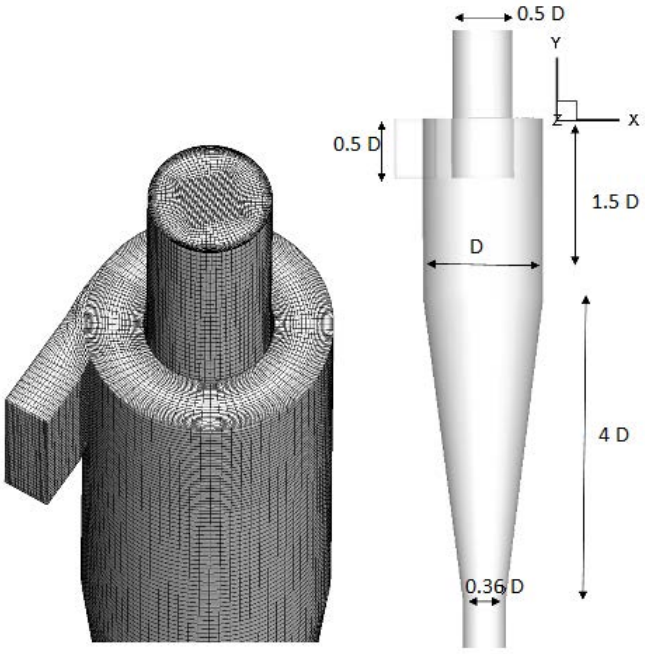

Figure 1: Geometry specifications and unstructured mesh of the stairmand cyclone(Slack *et al.*, 2000)

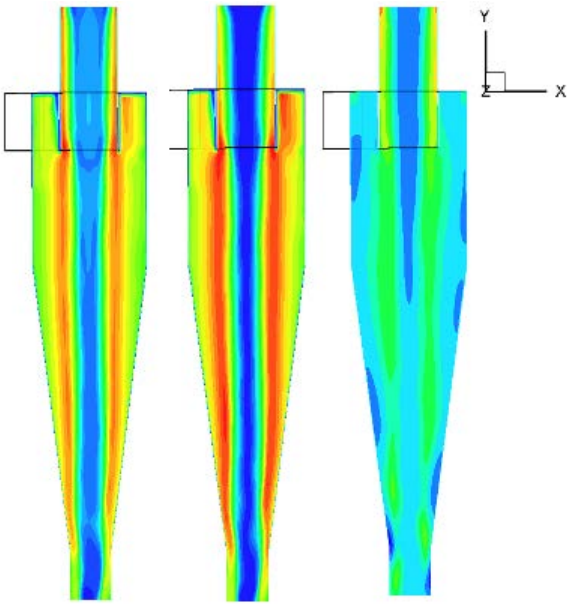

Figure 2: Contours of Left:Mean velocity magnitude(red is 40 m/s or higher and blue is 1 m/s or lower), Center: Mean tangential velocity (red is 36 m/s or higher and blue is 1m/s or lower) Right: Mean axial velocity (red is 20m/s or higher and blue is -10 m/s or lower)

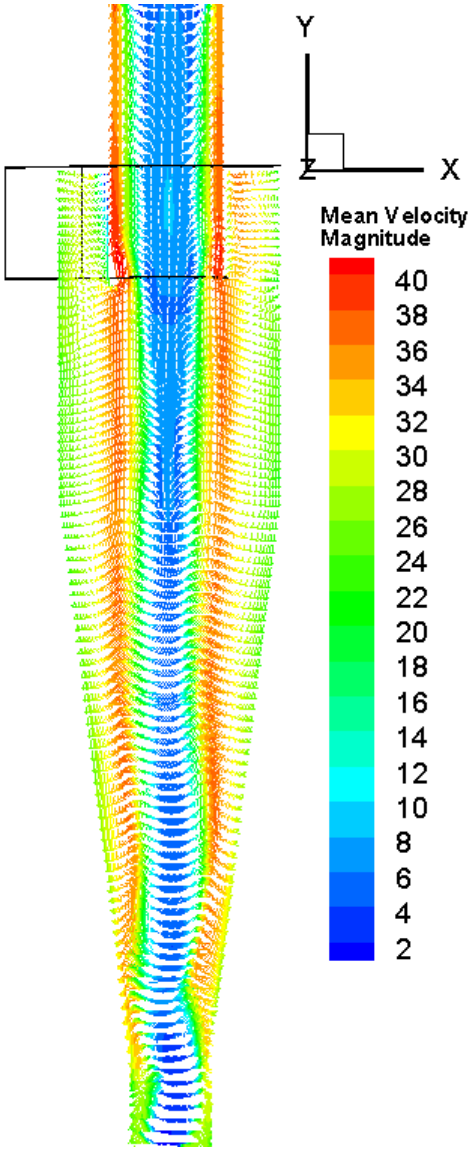

Figure 3: Velocity vectors for cyclone flow at feed air flow rate of $0.0203m^3$ colored by velocity magnitude

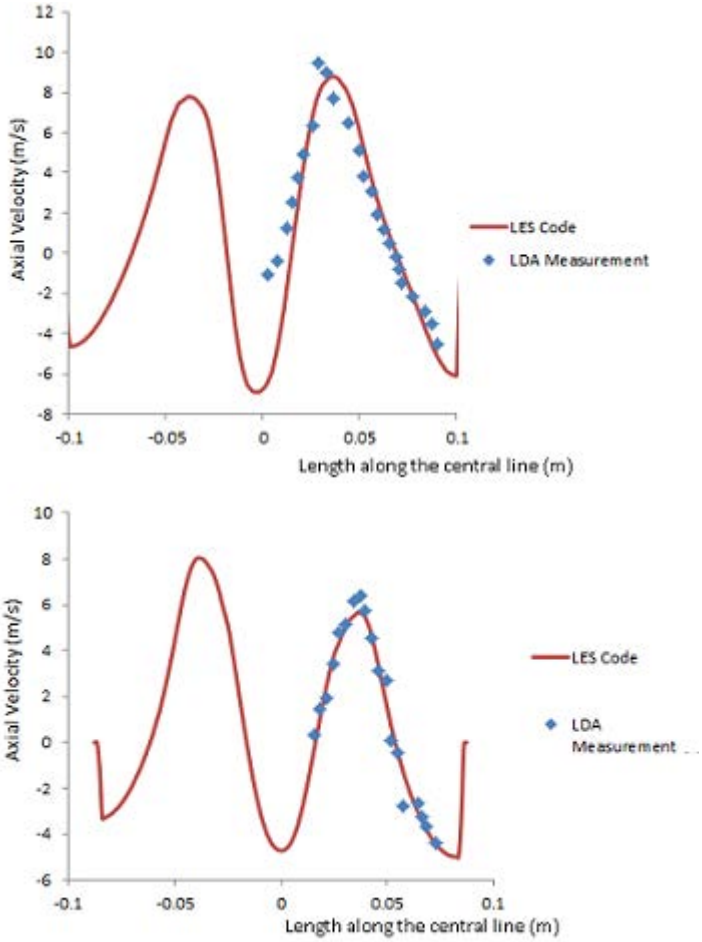

Figure 4: Comparison of axial velocity with LDA measurements from (Slack *et al.*, 2000) at left:0.38 m from top of the overflow and right: 0.59m from the top of the overflow

central core regions for such highly strained flows. The axial velocity profile show flow reversals near the central core region. Where the central core has downward flow towards the underflow while the region outside the central core has predominantly upward flow except near the walls where the flow is downwards towards the underflow. Similarly the tangential velocity also shows an increase in magnitude as we proceed from the walls towards the center reaching a maximum at a region where flow reversal start to take place and the tangential component reduces to a minimum value close to zero near the center. The comparison of the mean axial velocity and tangential velocity along the center line with the LDA measurements reported in (Slack *et al.*, 2000) for two different axial location are given in figure 4 and 5 respectively. Good quantitative comparison for the two velocity components at stations located at 0.38 m from the top and at 0.59 m from the top can be observed between the LES simulated value and the experimental results.

Phase segregation in a hydrocyclone

The multiphase code is tested for a poly dispersed slurry flow problem and study the phase segregation within the cyclone.As the algebraic slip mixture multiphase solver has not been successfully tested for higher density ratio, air core free design from (Vakamalla *et al.*, 2017) having a rod along the central core is chosen for the study. The geometry and the unstructured grid containing around 5×10^5 hexahedral cells is shown in figure 6.

Water with density 998.1 kg/m^3 and viscosity 0.00103 kg.

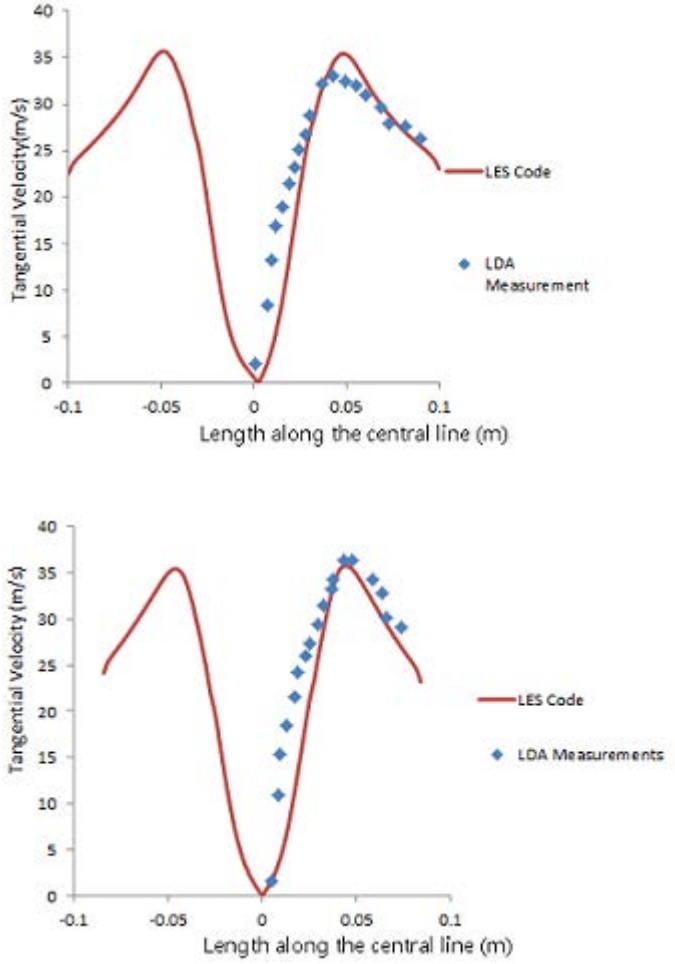

Figure 5: Comparison of tangential velocity with LDA measurements from (Slack *et al.*, 2000) at left:0.38 m from top of the overflow and right: 0.59m from the top of the overflow

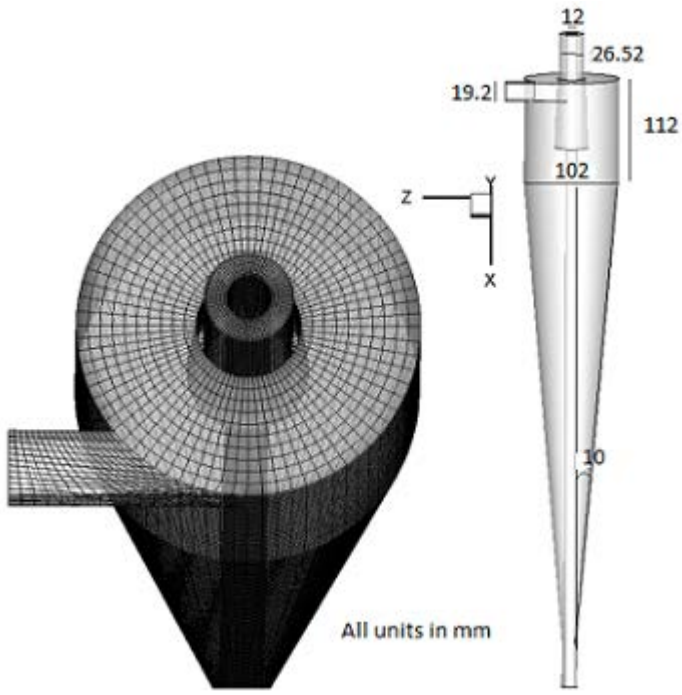

Figure 6: Geometry specifications and unstructured mesh prepared for the cyclone similar to (Vakamalla *et al.*, 2017)

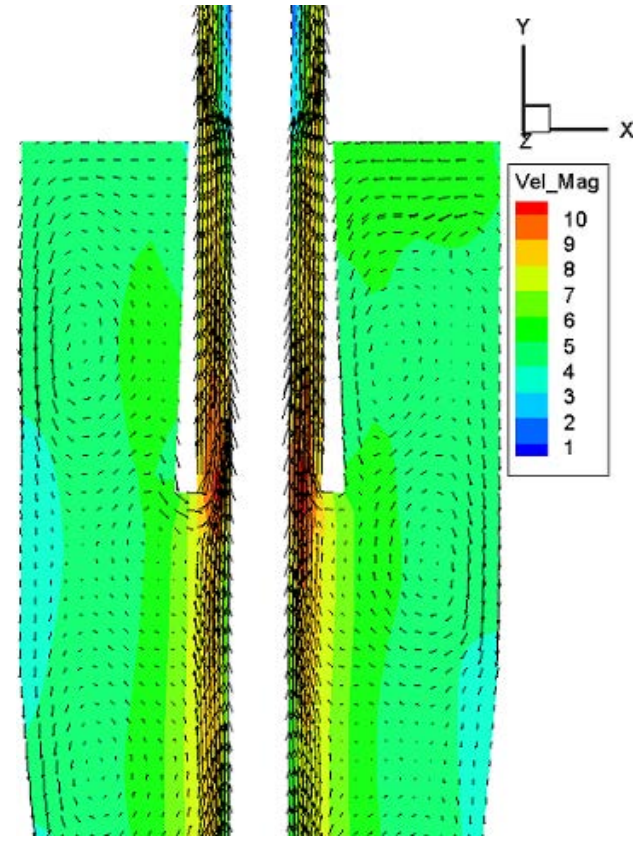

Figure 7: Vector plot for the slurry flow

Figure 8: Iso surface for contour level 0.005 volume fraction for phases left to right: phase 6 to phase 1

Figure 9: Iso surface for contour level 0.01 volume fraction for phases left to right: phase 6 to phase 1

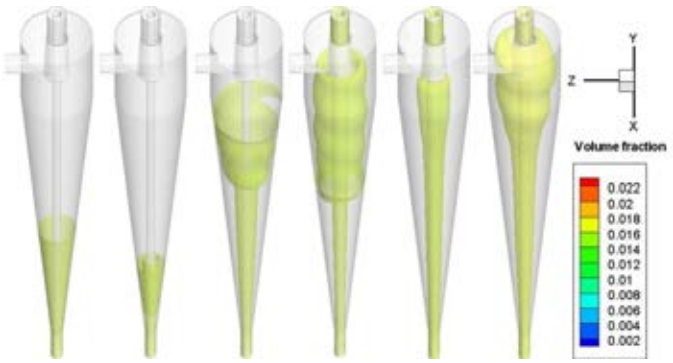

Figure 10: Iso surface for contour level 0.015 volume fraction for phases left to right: phase 6 to phase 1

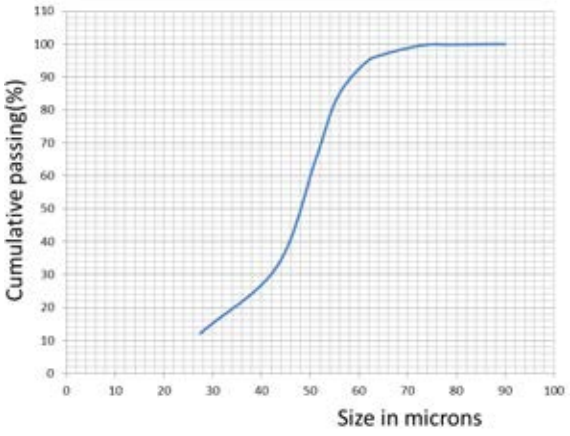

Figure 12: Particle classification curve for the air core free hydrocyclone design for water flow rate of 1.665 kg/m^3

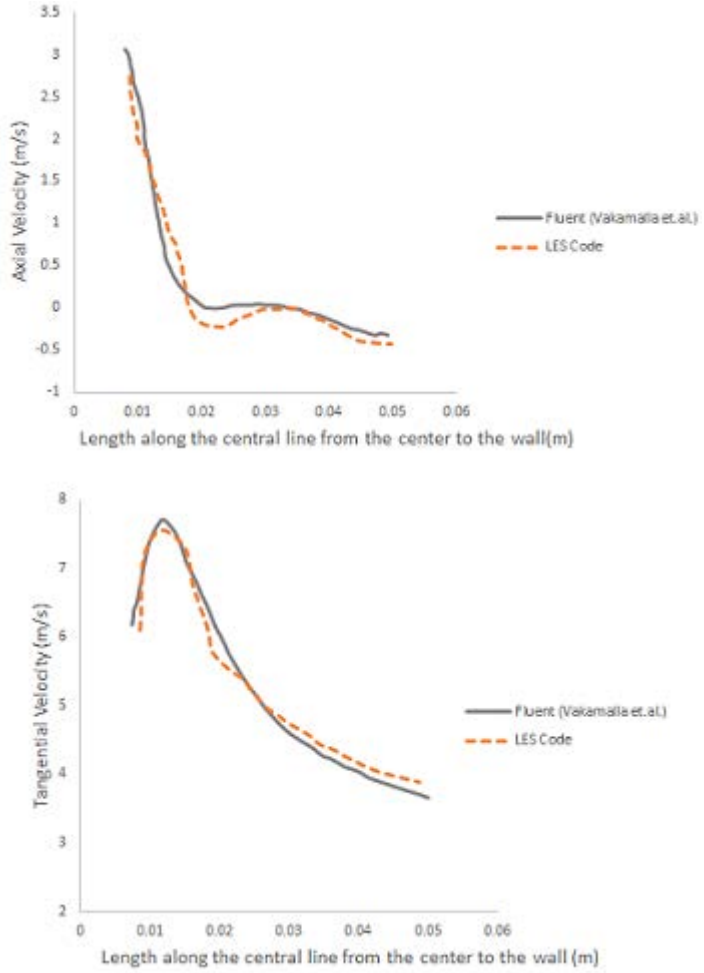

Figure 11: Comparison of left: Axial velocity and right: Tangential velocity at the mid plane along the line at the intersection of the conical and cylindrical sections

$m^{-1}s^{-1}$ is used as the continuous phase fluid. Varying sizes of silica powder with density 2650 kg/m^3 was used to specify the different secondary phases properties. The different phase size and volume fraction at the inlet is given in the table 1. Inlet flow rate of water was maintained at 1.664

Table 1: Phase size and distribution.

Phase	Diameter (μ m)	Feed Volume fraction
Phase 1	3.35	0.0174
Phase 2	10.25	0.0124
Phase 3	19.37	0.01158
Phase 4	28.27	0.00509
Phase 5	38	0.01329
Phase 6	68	0.00252

kg/s. Both the overflow and the underflow are specified gauge pressure values and the velocities and phase fractions were specified homogeneous neumann boundary conditions. The central rod was specified with no slip wall boundary condition. The secondary phase was introduced after the steady state velocity profile for the single phase water flow is obtained. The velocity magnitude profile at the mid plane for the single phase flow and the comparison of results with the fluent simulation performed in the study(Vakamalla *et al.*, 2017) is presented in the figure 11. The slurry flow patterns can be visualized using the vector plots given in figure 7 along the mid plane parallel to the inlet flow direction. Plots show the central region of positive axial velocity towards the overflow while minor circulations near in the central region. The phase segregation is studied using the iso contour for three different concentration. The low concentration contour at volume fraction value 0.005 is given in figure 8. The contour show that the smallest size fraction is more evenly distributed with very small regions near the overflow having smaller concentration. The regions of low concentration for the larger phases changes from the central rod region to regions near the wall as the size increases. The medium and high concentration iso contour at level 0.01 and 0.015 are given in figure 9,10 respectively . The smallest phase medium concentration regions are still the central core region while similar trend of segregation towards the walls for larger sizes can be observed. The largest phase fraction is located mainly near the walls and the underflow. The high concentration iso contour plots show the evenly distributed

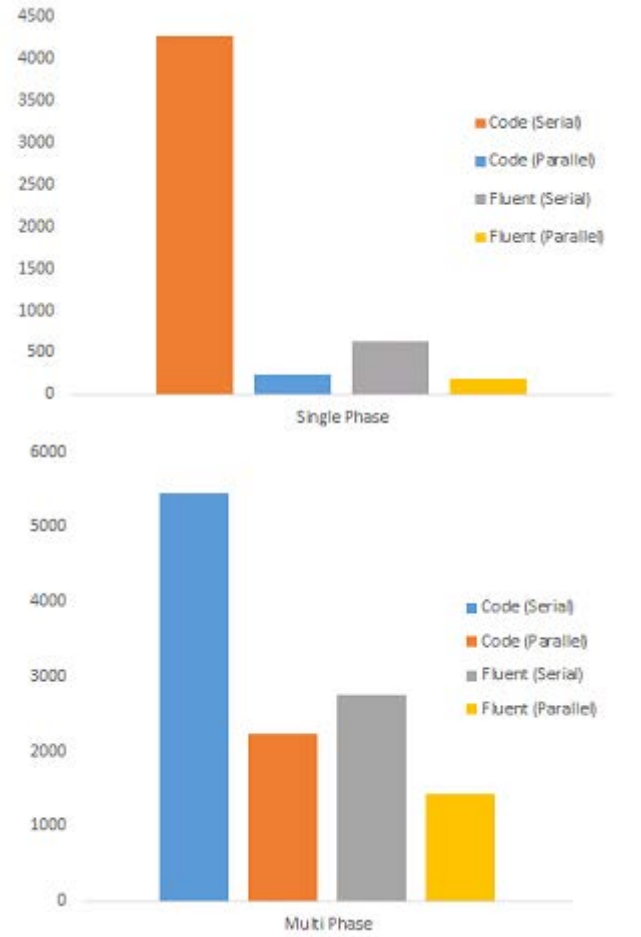

Figure 13: Comparison of time required in seconds for 100 timesteps of simulation

smallest size fraction. The cut-point for the said design was calculated using the particle efficiency curve given in figure 12 , which comes out to be 48.1 μm

Speed up obtained

The comparison of time required for the completion of 100 time steps of transient simulations due to the parallel GPU implementation with the serial implementation of the code along with the serial and parallel versions of commercial code Fluent is given in figure 13. The single phase parallel implementation reported speed up of around 11.3X over the serial code implementation. Compared to the serial version of fluent the speed up obtained is around 2.75 X. The code is performs slower as compared to the parallel version of fluent using 4 cores where a speed up of 1.6X is recorded for fluent parallel implementation over the parallel code. While for the multiphase implementation a speed up of 2.3X is obtained for the parallel implementation of the code over the serial one. Whereas, the speed up obtained over fluent serial implementation is 1.25X. The multiphase parallel implementation also performs slower as compared to the parallel implementation of fluent. Where the parallel fluent solver is reported to be 1.9 X faster than the parallel code implementation. This slower operation of the multiphase code as compared to the single phase solver is due to the amount of time expended on solving the phase tracking equations which is done on the CPU. The parallelisation of the solver for the phase tracking equation and the validation of the multiphase solver is the scope of the future work.

CONCLUSION

The development of an unstructured LES multiphase solver was presented for simulating highly strained slurry flows. Algebraic slip model was used to model the poly-dispersed slurry system. Where local velocity fields cause phase segregation due to varying inter phase momentum exchange due to drag and lift based on size of the particle. The solver is tested for single phase cyclone flows and validated against LDA measurements provided in (Slack *et al.*, 2000). The multiphase implementation was tested for particle classification with hydrocyclone geometry suggested in (Vakamalla *et al.*, 2017). The velocity profiles and the cut point obtained from the predicted particle separation curve was similar to the one obtained using the same design in the reference. Implementation of GPU parallelization for the compute intensive LES methodology is presented and the speed up obtained for the parallel implementation is reported. The parallel solver makes it computationally feasible to conduct design explorations even at industrial configuration.

REFERENCES

BRENNAN, M.S. (2006). "CFD Simulations of Hydrocyclones with an Air Core: Comparison Between Large Eddy Simulations and a Second Moment Closure". *Chemical Engineering Research and Design*, **84(6)**, 495–505.

DALAL, A., ESWARAN, V. and BISWAS, G. (2008). "A Finite-Volume Method for Navier-Stokes Equations on Unstructured Meshes". *Numerical Heat Transfer, Part B: Fundamentals*, **54(3)**, 238–259.

DATE, A.W. (2005). "Solution of transport equations on unstructured meshes with cell-centered colocated variables . Part I : Discretization". *International Journal of Heat and Mass Transfer*, **48**, 1117–1127.

DAVIDSON, L. (1996). "A Pressure Correction Method for Unstructured Meshes with Arbitrary Control Volumes". *International Journal for Numerical Methods in Fluids*, **22**, 265–281. URL http://doi.wiley.com/10.1002/(SICI)1097-0363(19960229)22:4{%}3C265::AID-FLD359{%}3E3.0.CO;2-J.

DEARDORFF, J.W. (1970). "A numerical study of three-dimensional turbulent channel flow at large Reynolds numbers". *Journal of Fluid Mechanics*, **41(1970)**, 453. URL http://www.journals.cambridge.org/abstract{_}S0022112070000691.

GERMANO, M., PIOMELLI, U., MOIN, P. and CABOT, W.H. (1991). "A dynamic subgrid-scale eddy viscosity model". *Phys. Fluids A Fluid Dyn.*, **3(7)**, 1760. URL http://scitation.aip.org/content/aip/journal/pofa/3/7/10.1063/1.857955.

HAASE, G., LIEBMANN, M., DOUGLAS, C.C. and PLANK, G. (2010). "A parallel algebraic multigrid solver on graphics processing units". *Lecture Notes in Computer Science (including subseries Lecture Notes in Artificial Intelligence and Lecture Notes in Bioinformatics)*, **5938 LNCS**, 38–47.

HEGE, H.C. and STUBEN, H. (1991). "Vectorization and parallelization of irregular problems via graph colouring". *Proceedings of the 5th International Conference on Supercomputing*, 47–56.

KHOSLA, P.K. and RUBIN, S.G. (1974). "A diagonally dominant second-order accurate implicit scheme". *Computers and Fluids*, **2(2)**, 207–209.

KOBAYASHI, T. (1992). "Large eddy simulation of backward-facing step flow". *Communications in applied numerical methods*, **8(October 1991)**, 431–441.

LEONARD, A. (1975). "Energy Cascade in Large-Eddy Simulations of Turbulent Fluid Flows". *Turbulent Diffusion in Environmental Pollution Proceedings of a Symposium held at Charlottesville*, **Volume 18**, 237–248. URL http://www.sciencedirect.com/science/article/pii/S0065268708604641.

LILLY, D.K. (1992). "A proposed modification of the Germano subgrid-scale closure method". *Physics of Fluids A: Fluid Dynamics*, **4(3)**, 633.

MANNINEN, M. and TAIVASSALO, V. (1996). "On the mixture model for multiphase flow".

MOIN, P. and APTE, V. (2006). "Large-Eddy Simulation of Realistic Gas Turbine Combustors". *AIAA Journal*, **44(4)**, 698–708.

MOIN, P. and KIM, J. (1982). "Numerical investigation of turbulent channel flow". *Journal of Fluid Mechanics*, **118**, 341–377.

NARASIMHA, M., BRENNAN, M. and HOLTHAM, P. (2006). "Large eddy simulation of hydrocyclone prediction of air-core diameter and shape". *International Journal of Mineral Processing*, **80(1)**, 1–14. URL http://linkinghub.elsevier.com/retrieve/pii/S0301751606000032.

NARASIMHA, M., BRENNAN, M., HOLTHAM, P. and NAPIER-MUNN, T. (2007). "A comprehensive CFD model of dense medium cyclone performance". *Minerals Engineering*, **20(4)**, 414–426. URL http://www.sciencedirect.com/science/article/pii/S0892687506002494.

POPE, S.B. (2004). "Ten questions concerning the large-eddy simulation". *New Journal of Physics*, **6(1)**, 35.

REDDY, R. and BANERJEE, R. (2015). "Computers & Fluids GPU accelerated VOF based multiphase flow solver and its application to sprays". *COMPUTERS AND FLUIDS*, **117**, 287–303. URL http://dx.doi.org/10.1016/j.compfluid.2015.05.013.

SANDERS, J. and KANDROT, E. (2010). *CUDA by Example*, vol. 54. arXiv:1011.1669v3, URL http://wwwzb.fz-juelich.de/contentenrichment/inhaltsverzeichnisse/2010/9780131387683.pdf.

SLACK, M., PRASAD, R., BAKKER, A. and BOSYAN, F. (2000). "Advances in cyclone modelling using unstructured grids". *Chemical Engineering Research and Design*, **78(November)**, 1098–1104.

VAKAMALLA, T.R., KORUPROLU, V.B.R., ARUGONDA, R. and MANGADODDY, N. (2017). "Development of novel hydrocyclone designs for improved fines classification using multiphase CFD model". *Separation and Purification Technology*, **175**, 481–497.

XU, C., DENG, X., ZHANG, L., FANG, J., WANG, G., JIANG, Y., CAO, W., CHE, Y., WANG, Y., WANG, Z., LIU, W. and CHENG, X. (2014). "Collaborating CPU and GPU for large-scale high-order CFD simulations with complex grids on the TianHe-1A supercomputer". *Journal of Computational Physics*, **278**, 275–297. URL http://www.sciencedirect.com/science/article/pii/S0021999114005786.